Tree Physiology Advance Access published July 15, 2014

Tree Physiology 00, 1–15
doi:10.1093/treephys/tpu049

Research paper

On the causes of rising gross ecosystem productivity in a regenerating clearcut environment: leaf area vs. species composition

Myroslava Khomik[1], Christopher A. Williams[1,3], Melanie K. Vanderhoof[1], Richard G. MacLean[1] and Sophie Y. Dillen[2]

[1]Graduate School of Geography, Clark University, 950 Main Street, Worcester, MA 01610, USA; [2]Biology Department, Antwerp University, Research Group Plant and Vegetation Ecology, Universiteitsplein 1, 2610 Wilrijk, Belgium; [3]Corresponding author (cwilliams@clarku.edu)

Received December 20, 2013; accepted May 15, 2014; handling Editor Michael Ryan

Clearcutting a forest ecosystem can result in a drastic reduction of stand productivity. Despite the severity of this disturbance type, past studies have found that the productivity of young regenerating stands can quickly rebound, approaching that of mature undisturbed stands within a few years. One of the obvious reasons is increased leaf area (LA) with each year of recovery. However, a less obvious reason may be the variability in species composition and distribution during the natural regeneration process. The purpose of this study was to investigate to what extent the increase in gross ecosystem productivity (GEP), observed during the first 4 years of recovery in a naturally regenerating clearcut stand, was due to (i) an overall expansion of leaf area and (ii) an increase in the canopy's photosynthetic capacity stemming from either species compositional shifts or drift in physiological traits within species. We found that the multi-year rise in GEP following harvest was clearly attributed to the expansion of LA rather than a change in vegetation composition. Sizeable changes in the relative abundance of species were masked by remarkably similar leaf physiological attributes for a range of vegetation types present in this early-successional environment. Comparison of upscaled leaf-chamber estimates with eddy-covariance-based estimates of light-response curves revealed a broad consistency in both maximum photosynthetic capacity and quantum yield efficiency. The approaches presented here illustrate how chamber- and ecosystem-scale measurements of gas exchange can be blended with species-level LA data to draw conclusive inferences about changes in ecosystem processes over time in a highly dynamic environment.

Keywords: chamber-based gas exchange method, eddy-covariance method, forest disturbance and regeneration, forest ecophysiology from leaf to canopy, leaf area index, upscaling.

Introduction

Forests occupy ~30% of the terrestrial land surface (FAO 2006) and absorb roughly 59 Pg of carbon from the atmosphere on an annual basis (Beer et al. 2010), representing ~49% of the total annual gross primary productivity on earth (Denman et al. 2007). Due to forests' potential to act as sinks for rising atmospheric CO_2 (Myneni et al. 2001, Goodale et al. 2002), interest in the dynamics of a forest's carbon cycle has piqued in recent decades (Bonan 2008). The sink capacity of a forest ecosystem depends on a range of factors, including climate (Nemani et al. 2003), species composition (Kirby and Potvin 2007), stand age (Pregitzer and Euskirchen 2004), site quality (Oren et al. 2001), site management (Jandl et al. 2007, Finkral and Evans 2008) and disturbance events (Amiro et al. 2010). Disturbances, such

as fires (Dixon and Krankina 1993, Amiro et al. 2001, Bond-Lamberty et al. 2007), harvest (Keenan and Kimmins 1993), herbivory (Kielland and Bryant 1998), ice storms (Hooper et al. 2001, Rustad and Campbell 2012), insect infestations and pathogens (Hicke et al. 2012), pollution (Kozlowski 1980) and windfall (Everham III and Brokav 1996), have varying degrees of severity, perturbing the forest carbon cycle in unique ways.

Clearcutting is one of the most severe disturbances to the carbon uptake of forested ecosystems, requiring 10 years or more for the system to recover its carbon sink capacity (Amiro et al. 2010). While the initial recovery of productivity after a clearcut at the site can be attributed to increasing leaf area index (LAI; Humphreys et al. 2005, Bracho et al. 2012, Coursolle et al. 2012), changes in the composition of vegetation at the site, with time, are also likely to occur (Bazzaz 1979, Keenan and Kimmins 1993). Given that some species have higher rates of photosynthesis compared with others (Dillen et al. 2012), the overall increase of the site's CO_2 uptake could be, in part, due to this changing vegetation composition.

A number of studies have examined the dynamics of clearcut regeneration. Many used the chronosequence approach, simultaneously comparing sites of similar stand composition and growing in similar environments, but of varying age (Amiro et al. 2010, Canadian Carbon Program 2011). Fewer studies have followed the dynamics of regeneration for a single site from the time of clearing to maturity (Likens et al. 1978). Furthermore, while past studies have looked at initial stages of regeneration, showing a steady increase in gross ecosystem productivity (GEP), we are unaware of any study documenting the underlying cause of this initial rise of GEP in a temperate, deciduous broadleaf forest environment, other than vegetation regeneration and expansion.

This study reports a detailed physiological study of a small (8 ha) clearcut located in the Harvard Forest Long-Term Ecological Research site in central Massachusetts, USA. Such clearcuts are not common in central Massachusetts, comprising <10% of all harvested lands (Kittredge et al. 2009, Twibell and Williams 2011), but clearcutting is more common regionally (Smith et al. 2009) and the practice is expected to increase in the future (Becker et al. 2009). Implications for regional carbon, water and energy budgets and dynamics have received relatively little attention, but have been the subject of intensive monitoring and measurement at the Harvard Forest clearcut site, where we have documented a rapid increase in GEP within the first 4 years of regeneration (Williams et al. 2014). The purpose of this study was to identify the leading cause of the observed multi-year rise in productivity in the first 4 years of recovery: (i) an overall expansion of the leaf area (LA) or (ii) changes in vegetation composition toward species with higher photosynthetic capacity. We combined measurements of species composition and LA, species-specific rates of photosynthesis and ecosystem-scale GEP, measured over the first 4 years post-clearcut.

Materials and methods

Site location and description

The study site occupies roughly a 200 × 400 m^2 area (8 ha) near the top of Prospect Hill (42.546N, 72.174W, elevation 403 m) within the Harvard Forest Long-Term Ecological Research Site, in Petersham, MA, USA. Prior to the clearcut in the autumn of 2008, the site was a white spruce (*Picea glauca*) and Norway spruce (*Picea abies*) plantation that was established between 1916 and 1937. Large amounts of coarse woody debris were left behind at the site after the harvest (Vanderhoof et al. 2013). Regeneration of vegetation at the site after the harvest was rapid, with over 20 different species identified during the first year of surveying (see Table S1 available as Supplementary Data at *Tree Physiology* Online). Seedlings reached an average height of 1.4 ± 0.8 m by 2012 (three growing seasons post-clearing) with a stem density averaging 29,000 tree stems per hectare. Following the US Soil Taxonomy, the soil at our site is classified as a well-drained Spodosol, of the Typic Haplorthod great group, characterized by coarse-loamy texture with a subsurface illuvial layer (NRCS 2010). The mean annual temperature at Harvard Forest is 7.8 ± 0.8 °C and the mean annual precipitation is 972 ± 171 mm, based on a 30-year record from 1980 to 2012 collected at the local weather station (Boose 2001). This estimate of precipitation may underestimate contributions from snow. Additional site details are presented in Williams et al. (2014).

Tower flux and meteorological data

Since mid-June of 2009, the site has been instrumented with a 3D sonic anemometer (CSAT3, Campbell Scientific, Logan, UT, USA) and an open-path infrared gas analyzer (IRGA, LI-COR LI-7500, Lincoln, NE, USA) located above the canopy on a 5-m-tall tripod tower to measure the fluxes of carbon, water, energy and momentum between the land surface and the atmosphere. Eddy-covariance instruments were installed at 3.0–5.5 m and elevated annually during May–June to maintain a measurement height at or >1.5 times the canopy height. High-frequency (10 Hz) wind speed, air temperature, water vapor concentration and CO_2 concentration were recorded and processed into half-hourly turbulent fluxes of water vapor, sensible heat, momentum and CO_2. Half-hourly incoming and outgoing longwave and shortwave radiation fluxes were measured with a Kipp and Zonen (Delft, The Netherlands) CNR1 radiometer. Photosynthetically active radiation (PAR, μmol m^{-2} s^{-1}) was recorded with a quantum sensor (LI-190SB, LI-COR). Air temperature and humidity were recorded with a shielded, solid-state sensor at 2.5-m height (Vaisala HMP45C, Campbell Scientific). Volumetric soil water content (θ, m^3 H_2O m^{-3} soil) was measured with 15-cm-long frequency domain reflectometry probes (CS615, Campbell Scientific), installed horizontally in the soil at two separate locations, at the following depths:

10, 25, 50 and 94 cm, or 10, 20, 40 and 80 cm. Soil temperature (T_s) was measured with spatially averaging soil thermocouple probes (TCAV, Campbell Scientific), installed at 2 and 8 cm below the ground surface and within 2 m of soil moisture probes. Meteorological measurements were averaged into half-hourly intervals during analysis.

Precipitation data shown in this manuscript were obtained from the Fisher Meteorological Station (Boose 2001), located in an open field on the Harvard Forest property. Daily precipitation was measured with a Met One 385 heated rain gauge (Campbell Scientific; top of gauge 1.6 m above the ground). Although heated, such precipitation gauges are prone to underestimating the amount of snowfall.

Raw, high-frequency eddy-covariance (EC) data were filtered to remove data spikes from instrument errors, followed by further post-processing to calculate 30-min net CO_2 flux estimates and involving additional data filtering to ensure a footprint representative of the clearcut target, avoid low turbulence conditions and remove wind sectors that sample the clearcut target poorly. Data gaps were filled with the marginal distribution sampling approach of Reichstein et al. (2005), retaining only those data filled with high confidence regarding quality. Measured net ecosystem CO_2 exchange was separated into ecosystem respiration (R_{eco}) and GEP using the approach of Reichstein et al. (2005), as well as an alternative approach of Lasslop et al. (2010). We found that, while the Lasslop et al. (2010) method produced GEP values that were consistently 12–20% lower compared with GEP values produced by the Reichstein et al. (2005) method, the overall rise and trends in GEP across the years and months were comparable between the methods (data not shown). Therefore, for the purpose of this study, we used the Reichstein et al. (2005)-derived GEP values. For full details on site instrumentation and flux data processing, see Williams et al. (2014).

Ecosystem-level light-response curves from tower-generated data were produced, for the years 2010 and 2012, separately, as follows. Using half-hourly data collected only from May to September of each respective year, PAR values were averaged to the nearest 10 for PAR levels up to 100 μmol m^2 s^{-1} and to the nearest 100 for PAR levels >100 μmol m^2 s^{-1} to define data bins over a range of light levels. Within each light level, we calculated statistics (mean and standard deviation) of the corresponding gap-filled GEP fluxes.

Vegetation surveys

Ground cover and vegetation composition Ground cover was recorded using the line-intercept method along five 50-m-long transects radiating from the flux tower into the surrounding clearcut area. Surveys were conducted annually from 2010 to 2013 at the beginning of June and in July, and included records of vegetation to the species level, bare soil, rocks, stumps and coarse woody debris. The ground cover of each object i (i.e., vegetation, bare soil, rocks, woody debris, stumps) was calculated as

$$\%\ \text{ground cover}\ i = \frac{\text{width}\ i\ (\text{cm})}{25{,}000\ \text{cm}} \times 100\%, \quad (1)$$

where width is the total sum of measured widths of i occurring along all five transects (5 × 50 m). Note that overlap of vegetative strata allows the sum of all ground cover to exceed 100%. Data analysis involved aggregation into cover-type groups, including vegetation types (i.e., herbs, shrubs and trees), bare soil, rocks, stumps and debris. Each group's *relative contribution* to total ground cover was calculated as the ratio of the group's ground cover to the overall site's ground cover within a given year.

To assess relative changes in vegetation composition, the percentage of total vegetation cover for any species j crossing the line intercept was calculated:

$$\%\ \text{vegetation cover}\ j = \frac{\text{width}\ j\ (\text{cm})}{\sum_{j=1}^{j=n} \text{width}\ j\ (\text{cm})} \times 100\%, \quad (2)$$

where width is the total width of the jth species from all five transects and n denotes the number of different species sampled. Data from June and July surveys in each year were combined to provide annual statistics.

Leaf area by species Species-specific leaf area (SLA, projected, one-sided LA per ground area occupied by an individual plant of a particular species) was sampled for a select number of species by destructive sampling (see Table S2 available as Supplementary Data at *Tree Physiology* Online). Two to five representative individuals of each species were selected. To minimize the method's impact, the number of individuals destructively sampled was based on the prevalence of the species within the study area. Individuals were chosen to represent the size spectrum observed along the vegetation transects. The aerial ground coverage of each individual was estimated using two tape meters placed perpendicular to each other and estimating the enclosed square, oval or triangular shape occupied by the individual. This method can lead to underestimation of aerial ground cover if the shade outline of the plant was not within the square, or to overestimation if the plant's outline was smaller than the square outline. We assume that these two errors in estimation would cancel each other out when sampling several individuals.

Each individual was destructively sampled by removing all the green leaves from the individual. Total (one-sided) LA was determined by scanning the leaves in the laboratory, using a LI-3000 leaf area meter (LI-COR). The scanned LA was divided by the ground area occupied by the individual plant, to produce

a leaf area estimate (LA) for the species. This value was used to calculate species-specific LAI from the line-intercept vegetation cover, as described below.

Litterfall collection In August 2012, we deployed 25 litter traps across the site along the five transects used for the line-intercept survey. The traps were square frames, constructed out of wood planks: either 70 × 70 cm^2 (0.490 m^2 in area) or 30.48 × 30.48 cm^2 (0.372 m^2) in dimension, with fine-mesh window screening stapled over the bottom of each frame. Traps were placed close to the ground to maximize capture of falling shrub foliage, while still elevated to avoid ground contact and associated stimulation of decomposition. Litter in the traps was collected on a biweekly basis, starting from 20 September 2012 until 17 November 2012, and air dried in the laboratory. Each bag's litter was sorted by species, separating out intact foliage. Unidentifiable leaf samples, fruits, twigs, dead insects and seeds were placed into an aggregate 'other' subsample. Each identified foliar species subsample was weighed and this weight was used to calculate the site LAI for 2012, with the corresponding SLA, according to Eq. (5) shown below.

Leaf physiology Specific leaf area Specific leaf area (in $cm^2\ g^{-1}$) was estimated for the 10 most abundant species (Table 1), present in both years when SLA was sampled (i.e., 2010 and 2012). These species represented some 80% of the vegetation in year 2012 (Table 1 and see Table S1 available as Supplementary Data at *Tree Physiology* Online).

More than 100 leaves were sampled for each species in August of 2012. Leaves were collected randomly along the five transects used for vegetation line-intercept measurements and analyzed within 2 days of collection. Individual leaves were scanned on the LI-3000 leaf area meter (LI-COR) and their area (in cm^2) recorded. Scanned leaves were oven-dried for 48 h (at 60 °C). Dried leaves were weighed on a digital balance and SLA was calculated for each leaf as follows:

$$\mathrm{SLA} = \frac{\text{area (cm}^2\text{)}}{\text{weight (g)}}, \qquad (3)$$

where area is the one-sided projected LA of a single leaf and weight is the dry weight of that leaf. A mean across all leaves sampled, for each species sampled, was used in LAI calculations from the litter-trap data, as described below.

Leaf-scale photosynthesis measurements From June to September in 2010 and from the end of May to July in 2012, leaf-scale photosynthesis was measured on select, sun-lit leaves across a number of species (see Table S3 available as Supplementary Data at *Tree Physiology* Online) with a portable open-path gas exchange measurement system (LI-6400, LI-COR).

Light-response curves were measured by clamping a 2 × 3-cm^2 chamber onto a healthy, sun-lit leaf at the top to mid-level of the canopy, under a constant CO_2 of 380 ppm (using the 6400-01 CO_2 Injector from LI-COR); chamber air temperature was set to reflect outside ambient conditions, within ±5 °C; flow was set to a constant water mole fraction targeting the value that was established on the clamped leaf prior to the beginning of the response-curve measurement. Net photosynthesis (A_{net}) was logged at each set light-level, in replicates of three that were later averaged to give a single reading per light level, prior to further analysis. In 2012, the following light levels were sampled, by adjusting PAR levels inside the chamber with the red–blue light source (6400-2B LED light source, LI-COR): 1800, 1200, 1000, 800, 600, 400, 200, 50 and 0 (in μmol $m^{-2}\ s^{-1}$). For the zero-PAR setting, the light source was switched off and the branch containing the sampled leaf was shaded with a dark cloth. Intercellular CO_2 concentration (C_i) was allowed to stabilize before logging the measurement at a given light setting. After measurement, the leaf was detached and transported back to the laboratory for further analysis. Leaves that did not occupy the full area of the 2 × 3-cm^2 chamber were scanned in the laboratory for leaf area. During the 2010 measurement campaign, readings were taken at the following light levels: 1400, 1200, 1000, 800, 600, 400, 200, 100, 50, 40 and 0 μmol $m^{-2}\ s^{-1}$.

For the CO_2-response curves, similar procedures were used as for the light-response curves, except that the light inside the chamber was maintained at a constant level of 1800 μmol $m^{-2}\ s^{-1}$, while the following CO_2 concentration settings in the reference cell were cycled: 380, 100, 50, 380, 380, 500, 800 and 1000 ppm. During the 2010 measuring campaign, the following instrument settings were used: chamber CO_2 concentrations were set to 380, 180, 100, 70, 45, 380, 600, 720, 1000 and 2000 ppm; chamber temperature was set to 25 °C; the light inside the chamber was set to 1500 μmol $m^{-2}\ s^{-1}$; and the chamber relative humidity was maintained between 50 and 80%.

For the instantaneous photosynthesis survey measurements, three replicate individuals for 10 dominant plant species were selected and marked. During the 2012 measuring campaign, the same leaves were re-measured throughout the season, unless the leaf was damaged or browsed in between measurement dates, at which point the leaf was replaced by a new sample. During the 2010 measuring campaign, leaves were harvested at the end of the day. During measurements, light inside the chamber was set to match that outside, as recorded by the external PAR sensor. Leaf temperature was set to that of the leaf being measured at the beginning of the measurement period. Flow was set to ~500 μmol s^{-1} and sample CO_2 was set to 380 ppm. Once photosynthesis and conductivity stabilized, three replicate readings were taken, within 2–3 min, which were averaged before further analysis. The survey was performed twice a day, once in the morning and once in the afternoon, weather permitting. Survey measurements were performed on

Table 1. Some key physiological characteristics of select vegetation species sampled in 2010 and 2012 at our clearcut site. Mean values with the same superscript letter are not statistically different at the 95% confidence level. Numbers in parentheses indicate sample size used to calculate the associated statistic.

Scientific name	Common name	Short code	% Vegetation cover 2010[1]	% Vegetation cover 2012[1]	% Ground cover 2010[1]	% Ground cover 2012[1]	SLA ($cm^2\ g^{-1}$)	Leaf N % weight	Species LAI 2010 line intercept	Species LAI 2012 line intercept	Species LAI 2012 litter traps	A_{max} 2010[2]	A_{max} 2012[2]	Quantum yield Φ 2010	Quantum yield Φ 2012	$V_{cmax.25}$ 2010[2]	$V_{cmax.25}$ 2012[2]
Herbaceous[1]			10.9 ± 4.1	13.4 ± 3.3	10.9 ± 2.4	26.9 ± 9.8			0.05	0.11	0.09 ± 0.03						
Aralia nudicaulis	Wild sarsaparilla	Ws	0.3 ± 0.2	1.0 ± 0.8	0.3 ± 0.4	1.8 ± 1.2	279.6 ± 80.8[a] (142)		0.00 ± 0.0	0.01 ± 0.01							
Dennstaedtia punctilobula	Hay-scented fern	Hf	3.7 ± 4.0	6.6 ± 2.9	3.8 ± 2.0	13.6 ± 8.5	120.3 ± 23.2 (9)	2.3 ± 0.3[a] (2)	0.01 ± 0.10	0.05 ± 0.03	0.06 ± 0.01	9.4 ± 0.5[ab] (2)		0.041 ± 0.005[b] (2)		40 ± 0.3[b] (2)	
Polygonum sp.	Knotweed	Kw	6.9 ± 0.9	5.7 ± 1.2	6.8 ± 1.2	11.5 ± 4.7	296.9 ± 98.3[a] (139)	2.3 ± 0.4[a] (12)	0.03 ± 0.01	0.06 ± 0.02	0.04 ± 0.01		12.0 ± 3.3[a] (6)		0.0058 ± 0.017[ab] (6)		
Shrubs[1]			40.9 ± 3.1	38.2 ± 1.8	39.8 ± 0.8	75.0 ± 16.1			0.25	0.45	0.30 ± 0.06						
Rubus allegheniensis	Blackberry	Bb	36.3 ± 3.0	28.8 ± 1.8	35.4 ± 0.2	56.8 ± 15.7	221.2 ± 56.9[b] (182)	2.5 ± 0.6[a] (25)	0.23 ± 0.0	0.37 ± 0.10	0.25 ± 0.06	11.3 ± 4.0[a] (12)	11.9 ± 3.8[a] (7)	0.059 ± 0.009[ab] (12)	0.038 ± 0.004[ab] (7)	99 ± 63[ab] (8)	80 ± 45[ab] (3)
Rubus idaeus	Raspberry	Rb	4.6 ± 0.9	9.4 ± 0.3	4.5 ± 0.7	18.3 ± 3.5	216.2 ± 55.8[b] (154)		0.02 ± 0.0	0.08 ± 0.02	0.06 ± 0.02						
Trees[1]			21.7 ± 1.7	31.9 ± 3.0	21.0 ± 1.2	62.4 ± 10.3			0.48	1.31	1.23 ± 0.04						
Acer rubrum	Red maple	Rm	8.6 ± 0.6	11.5 ± 2.3	8.4 ± 0.3	22.0 ± 0.5	145.6 ± 23.4[d] (207)	1.6 ± 0.3[b] (26)	0.24 ± 0.0	0.62 ± 0.01	0.40 ± 0.04	6.4 ± 1.5[b] (8)	7.0 ± 1.8[b] (7)	0.052 ± 0.006[b] (8)	0.057 ± 0.016[b] (7)	69 ± 20[b] (7)	63 ± 14[b] (3)
Betula sp.	Birches	Bi	0.3 ± 0.2	1.1 ± 0.6	0.1 ± 0.2	2.2 ± 1.3	178.5 ± 33.6[c] (336)	2.3 ± 0.2[a] (21)	0.00 ± 0.0	0.05 ± 0.20	0.19 ± 0.04					135 ± 36[ab] (18)	
Prunus pennsylvanica	Pin cherry	Pc	7.1 ± 0.4	15.0 ± 1.9	6.9 ± 0.3	29.7 ± 10.1	178.0 ± 27.0[c] (215)	2.5 ± 0.3[a] (28)	0.10 ± 0.0	0.44 ± 0.15	0.47 ± 0.07	13.7 ± 2.4[a] (11)	13.2 ± 4.3[a] (7)	0.064 ± 0.007[a] (11)	0.042 ± 0.010[a] (7)	118 ± 24[a] (6)	71 (1)
Prunus serotina	Black cherry	Bc	5.7 ± 1.5	4.1 ± 0.2	5.5 ± 1.0	8.0 ± 1.3	147.0 ± 18.7[d] (196)	2.0 ± 0.3[a] (22)	0.14 ± 0.02	0.20 ± 0.03	0.12 ± 0.02	12.3 ± 4.2[a] (8)	10.7 ± 3.5[a] (7)	0.061 ± 0.007[ab] (8)	0.049 ± 0.010[ab] (7)	107 ± 36[ab] (7)	133 ± 68[ab] (4)
Quercus rubra	Red oak	Ro	0.1 ± 0.1	0.2 ± 0.1	0.1 ± 0.3	0.5 ± 0.0	183.9 ± 47.0[c] (182)	2.1 ± 0.3[a] (22)	0.00 ± 0.0	0.01 ± 0.0	0.05 ± 0.02	11.1 ± 3.4[a] (10)		0.059 ± 0.008[ab] (10)		75 ± 41[b] (10)	

[1]The ground cover for each subgroup (i.e., herbaceous, shrubs and trees) is the sum of the species listed in this table, and not the total sum of all species in each group, likewise for vegetation cover and LAI. Species listed here represent 56 and 85% of the total ground cover in 2010 and 2012, respectively. For vegetation and ground cover and LAI from the line-intercept method, the means and standard deviations are based on two measurements: June and July of each year.
[2]A_{max} and $V_{cmax.25}$ in units of μmol CO_2 m^{-2} s^{-1}.

4 days in 2010 (15 June, and 8, 26 and 27 July) and on 6 days in 2012 (12, 15, 18 and 27 June, and 2 and 3 July).

Leaf nitrogen Select leaves from a number of species (Table 1) were dried in an oven at 60 °C for 48 h, ground with a mortar and pestle, packed and analyzed for nitrogen content. In 2010, leaf nitrogen was analyzed with a dynamic flush combustion method using a NC 2100 Soil Analyzer (Carlo Erba Strumentazione, Rodano, Italy). In 2012, samples were analyzed in a CHNOS Elemental vario micro-cube analyzer (Elementar Analysensystem, GmbH), located at Harvard Forest. Only leaves on which light- and CO_2-response curves were measured were collected and sampled for carbon and nitrogen contents.

Leaf area index determination

From the line-intercept method The percent ground cover of each species sampled (j) along the line intercept describes the amount of ground cover that species occupied at the site at the time of sampling. We multiplied this percentage by the corresponding LA for that species (obtained from destructive harvesting, as described above) to quantify species-specific LAI:

$$\mathrm{LAI}_j = \%\ \text{ground cover}_j \times \mathrm{LA}_j. \quad (4a)$$

Although the sum of all species-specific LAI values would have given us the total site-level LAI, we were not able to destructively sample examples of all species present along the transects. To account for the missing species, we weighted the sum of sampled species-specific LAI by the vegetation cover of the respective group, x (i.e., herbs, shrubs and trees). The result was the group-specific LAI (LAI_x):

$$\mathrm{LAI}_x = \sum_{j=1}^{n}\left(\frac{\mathrm{LAI}_j}{(\%\text{veg cover})_j} \times 100\%\right), \quad (4b)$$

where n denotes the number of different species sampled from each group, x.

Finally, the sum of weighted group-specific LAI values produced the overall total site LAI:

$$\mathrm{LAI}_{site} = \mathrm{LAI}_{herb} + \mathrm{LAI}_{shrub} + \mathrm{LAI}_{tree}. \quad (4c)$$

From litter-trap collection Given the deciduous nature of the foliage at our site, species-specific LAI was estimated by collecting fallen leaves with traps of fixed area, weighing the resulting foliage by species and multiplying this by the species-specific leaf areas:

$$\mathrm{LAI}_j = \frac{\mathrm{weight}_j \times \mathrm{SLA}_j}{10.12\ \mathrm{m}^2}, \quad (5)$$

where weight_j is the total dry weight of the foliage of species j (in grams, g) collected at the end of the growing season within all traps (i.e., 22 traps in total, equating to 10.12 m^2) and SLA_j is the mean specific LA of species j ($m^2\ g^{-1}$). Each species-specific LAI value was grouped into the three corresponding vegetation groups (x) and weighted to account for unsampled vegetation, following Eq. (4b). The final site-level LAI value was the sum of LAI values from each group: herb, shrub and trees, following Eq. (4c).

LAI-2000 sampling In late August 2012, site-level LAI was also estimated with the LAI-2000 Plant Canopy Analyzer (LI-COR) optical plant area meter. Measurements were performed along one of the five line-intercept transects, just below the canopy, along eight points, at dusk. A 45° angle cap was used and data were corrected accordingly. Two additional measurements were performed before and after the transect survey, but in an adjacent open area free of shading. The difference between the mean open and the mean transect value provided an estimate of plant area index (PAI) at our site. Measured PAI was translated to LAI, by correcting for branches sampled during our destructive harvesting campaign (described above for estimation of species-level leaf area, involving select patches of trees: red maple, *Acer rubrum* (6.6 m^2); pin cherry, *Prunus pennsylvanica* (9.7 m^2); and black cherry, *Prunus serotina* (11.1 m^2). During that sampling campaign, we took measurements with the LAI-2000 instrument before and after leaf harvest within each patch. The corresponding ratio of LAI to PAI in defoliated patches was used to correct the measured site-total PAI to provide just the portion related to leaves (i.e., LAI).

Upscaling photosynthesis from leaf scale to canopy

Leaf-level net assimilation was multiplied by the corresponding species-specific leaf area (LAI_j) to obtain species-specific A_{net} per ground area. Note that chamber-based measurements provide net assimilation, which includes dark leaf respiration (R_{leaf}, which is signed negatively for a release from the leaf), while tower-based assimilation values represent gross assimilation without dark leaf respiration. In our comparison of light-response curves, the upscaled chamber-based curves were adjusted to account for R_{leaf}, which was obtained from the zero-PAR measurements, to give the upscaled-GEP. The species-specific, site-level responses were summed across corresponding vegetation groups, x (i.e., herbaceous, shrubs and trees), for each light level. The summed-up curves were weighted to reflect the species sampled (n), compared with the total species present, per vegetation group (x):

$$\text{weighted}\, f\left(\text{upscaled GEP, PAR}\right)_{\text{year},x} = \left(\sum_{j=1}^{n} f\left(\{A_{net} - R_{leaf}\}, \text{PAR}\right)_j \times \frac{\text{total \%veg cover}}{\sum_{j=1}^{n} \%\text{veg cover}_j}\right)_{\text{year},x}. \quad (6)$$

The weighted curves were summed to provide an estimate of the ecosystem-scale light-response curve.

For the instantaneous survey measurements, upscaling was completed for each individual day separately. If morning and afternoon measurements were available for a given day, these two sets of measurements were averaged per species. Each species-specific A_{net} value was then multiplied by the species-specific LAI value, for each species j sampled, and corrected for R_{leaf} losses, to give upscaled-GEP_{day} by species. This species-specific upscaled-GEP_{day} was then weighted by the percentage of vegetation cover represented by all species sampled (n) that day:

$$\text{upscaled} - \text{GEP}_{\text{day}} = \left(\frac{\sum_{j=1}^{n} \left(\overline{A_{\text{net}} - R_{\text{leaf}}} \right)_j \times \text{LAI}_j}{\sum_{j=1}^{n} \%\text{veg cover}_j} \times 100\% \right)_{\text{day}} . \quad (7)$$

Comparisons of the instantaneous upscaled A_{net} measurement with half-hourly ecosystem-level GEP from the EC method were made, using tower data collected within 30 min of chamber-based measurements.

Note that we used two different LAI_j estimates, one from the line intercept and the other from the litter-trap data, to calculate two different upscaled-GEP_{day} values in the year 2012. The percentage of vegetation sampled in each day is shown in Table S4 available as Supplementary Data at *Tree Physiology* Online.

Curve fitting and data analysis

Measured light-response curves were fitted using a rectangular hyperbola model, following Hanson et al. (1987):

$$A_{\text{net}} = A_{\text{max}} - A_{\text{max}} \times \left(1 - \frac{R_{\text{d}}}{A_{\text{max}}} \right)^{1-(\text{PAR}/\Gamma)}, \quad (8)$$

where A_{net} (μmol of CO_2 m^{-2} s^{-1}) is net photosynthesis at a given light (PAR, μmol m^{-2} s^{-1}) level, A_{max} is maximum photosynthetic capacity at saturating light levels (μmol of CO_2 m^{-2} s^{-1}), R_d is the dark respiration rate of the leaf (μmol of CO_2 m^{-2} s^{-1}) and Γ is the light compensation point. Fitted curves for each species that were sampled are shown in Figure S2 available as Supplementary Data at *Tree Physiology* Online. The maximum quantum yield (Φ, in μmol of CO_2 per μmol PAR), which describes the number of CO_2 molecules absorbed per quantum of light absorbed, was calculated from the first derivative of the above equation (Hanson et al. 1987):

$$\Phi = \frac{A_{\text{max}}}{\Gamma} \times \left(1 - \frac{R_{\text{d}}}{A_{\text{max}}} \right) \times \ln \left(1 - \frac{R_{\text{d}}}{A_{\text{max}}} \right). \quad (9)$$

Data processing and analysis was performed with R-software (version 2.15.0), using the R-Studio user interface and also in Microsoft® Excel software (version 2010). The resulting fitted parameters represent photosynthetic yield at the leaf temperature of the measured leaf.

The maximum carboxylation efficiency (V_{cmax}) for select species at our site was calculated following Sharkey et al. (2007). In our analysis and comparisons, we used the temperature-corrected V_{cmax} values (i.e., $V_{cmax.25}$) available as output from the Sharkey et al. (2007) routine.

Results

Gross ecosystem productivity recovery after the clearcut

The recovery of GEP post-clearcut at our site was steady and rapid (Figure 1). Growing season uptake increased 1.2 times (16%) from 2010 to 2011 and 1.4 times (44%) from 2010 to 2012 (Figure 1). By 2012, total growing season (May to September) GEP reached 1351 g C m^{-2} $year^{-1}$. Similarly, when comparing the mean of daily GEP values from our upscaled survey measurements, using the line-intercept-derived LAI values for upscaling, the upscaled 2010 mean value was 12.9 μmol CO_2 m^{-2} s^{-1} ($n = 4$), while the upscaled 2012 mean value was 21.3 μmol CO_2 m^{-2} s^{-1} ($n = 6$)—a 65% increase from 2010 to 2012 (see Figure 4a). Climate over the course of these 4 years was relatively comparable, without any positive trends that could be potentially related to the rising GEP (see Figure S1 available as Supplementary Data at *Tree Physiology* Online).

Attributing the observed increase in GEP

Expansion of vegetation cover Vegetation cover increased rapidly in the first three growing seasons following forest clearing (Figure 2a). Within 3 years, bare ground, exposed rocks, stumps and woody debris were overgrown with vegetation. Overall, total ground cover increased 1.2 times (from 129 to 152%) in 2011 and 1.5 times (increased to 199%) in 2012 compared to 2010 (Figure 2a). The increase in LAI was more pronounced: estimated LAI increased 1.4 times from 2010 to 2011 (1.2 to 1.7 m^2 m^{-2}) and more than doubled by 2012 (increased to 2.5 m^2 m^{-2}) (Figure 3). The estimated LA at our site for the year 2012, from three different methods, ranged from 2.2 ± 0.2 to 2.9 ± 0.2 m^2 m^{-2}.

Changes in vegetation composition The relative contribution of each vegetation group to the overall increase in ground cover varied over the years (Figure 2b). Contributions from herbs remained relatively constant, comprising about a quarter of total ground cover over all 3 years (24–25%, Figure 2b). Contributions from shrubs increased 1.2-fold (32.7 to 40.7%) from 2010 to 2011, and remained relatively constant in 2012. In contrast, tree cover consistently increased in its contribution

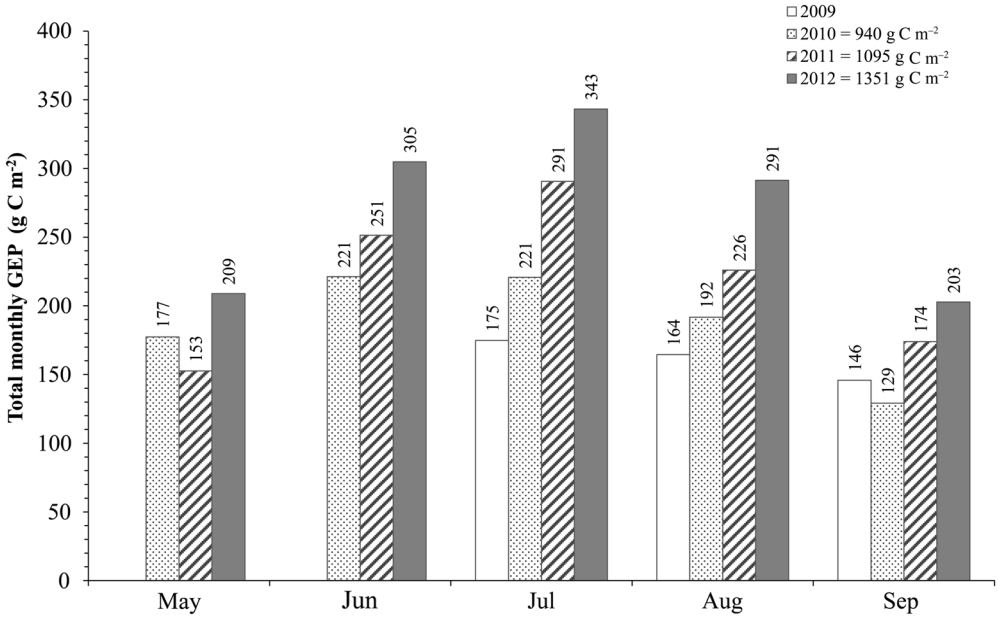

Figure 1. Monthly GEP for May to September across the 4 years of observation. Tower flux measurements began in mid-June of 2009. Total seasonal GEP values are listed next to each year in the legend. Gross ecosystem productivity clearly increased from 2010 to 2012, up by 16% from 2010 to 2011 and by 38% in 2012.

to total ground cover at the site—1.5-fold (17.6 to 25.8%) from 2010 to 2011 and twofold (17.6 to 35.1%) by 2012. Likewise, when considering LAI increases, the increase in tree LAI was by far the greatest of all the three groups from 2010 to 2012—a threefold increase according to the line-intercept-derived LAI (from 1.2 to 2.5 m^2 m^{-2}; Figure 3).

We also observed changes in species composition (between years) (Figure 2c). The abundance of herbs decreased somewhat during 4 years of the study (31.6 to 24.4%), while that of trees increased by up to 1.5-fold (23.3 to 35.8%). When considering the contribution of individual species to increasing vegetation cover from 2010 to 2012, pin cherry (*P. pennsylvanica*), birch (*Betula* sp.), red oak (*Q. rubra*) and red maple (*A. rubrum*) all increased substantially (Table 1 and see Table S1 available as Supplementary Data at *Tree Physiology* Online). There was also an initial shift from hay-scented fern (*D. punctilobula*) in 2009 to Allegheny blackberry (*R. allegheniesis*).

Variability in photosynthetic capacity Table 1 reports that maximum photosynthesis at saturating light levels (A_{max}), maximum quantum yield efficiency (Φ) and maximum rate of carboxylation (V_{cmax}) were all quite similar among the species tested (see Figure S4 available as Supplementary Data at *Tree Physiology* Online). This was consistent with the subtle variation in leaf nitrogen content across species (Table 1). These findings were true across a wide range of plant functional types, spanning herbaceous to woody plants. Red maple presented a noticeable exception to these broad patterns, with low photosynthetic capacity and low leaf nitrogen content relative to the other species (Table 1). There was also some separation of mean values across the remaining species, but these were not significantly different given the sizeable standard deviations around sample means for species.

In contrast to photosynthetic parameters, SLA differed statistically between the three major groups (herbs, shrubs and trees) and even among some trees (Table 1). Herbaceous vegetation tended to have larger SLA compared with shrubs, while trees had the lowest SLA. Overall, these findings suggest that changes in species composition did not appear to significantly shift photosynthetic capacity at the ecosystem level, and therefore the annual rise in GEP was not likely to have been driven by changes in photosynthetic rates over the past 4 years of recovery.

Changes in vegetation composition vs. expanded leaf area Direct comparison of leaf-upscaled GEP and tower-based instantaneous GEP showed good agreement for both 2010 and 2012 (Figure 4a). On uncommonly hot days, temperature and moisture at the surface of measured leaves inside the chamber were substantially hotter and drier than the conditions measured at the tower. On these days, sampled leaves were more stressed than what was typical for the whole canopy, leading to lower leaf-based estimates of assimilation. Vapor pressure deficit on those 3 days inside the chamber was about twice that outside of the chamber (data not shown), potentially leading to closed stomates.

We also compared GEP light-response curves from the tower with those derived from upscaled leaf-chamber measurements

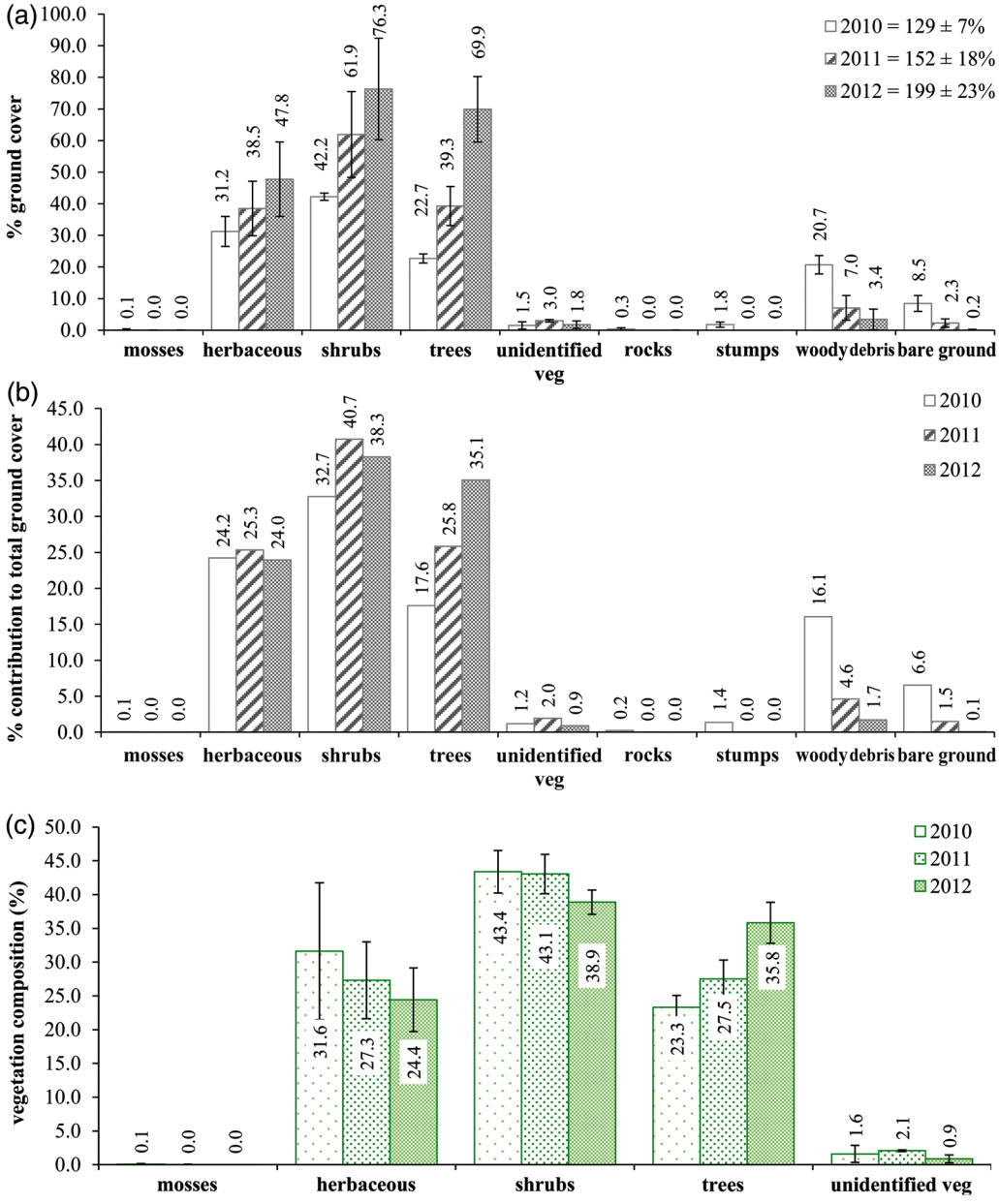

Figure 2. (a) Expansion of ground cover from 2010 to 2012 as measured with the line-intercept method during May to July of each year. Species overlap causes total ground cover to exceed 100% of the sampled length as indicated by totals reported in the legend; there was a steady increase in vegetation cover over the 4 years. However, not all vegetation types expanded equally. In (b), relative changes in the percent contribution of each cover type to total ground cover (i.e., normalized % ground cover, relative to total ground cover) are shown. The greatest change in ground cover was due to tree expansion. Changes in the site's canopy composition in the first few years of recovery are shown in (c). Clearly, despite the constant relative percent contribution of herbs to total ground cover during the 4 years of recovery, herbs' relative contribution to canopy composition decreased with time, at the expense of growing trees (c).

(Figure 5). The line-intercept approach resulted in somewhat larger GEP estimates due to methodological differences in estimating LAI (line-intercept vs. litterfall). Yet the two methods produced a range of leaf-based estimates of GEP that bracketed the maximum flux-tower-derived GEP values at high light levels (Figure 5). The shape of the leaf-upscaled estimates of GEP also reflected well the initial rise and slope of the tower values for both years (Figure 5). At low light levels, up to ~250 µmol the curves do match up well. However, tower-based response curves did not exhibit the same saturation at intermediate to high light levels as seen in leaf-based light-response curves (Figure 5). The fit between the two curves in 2010 was better compared with that in 2012, due to lower canopy stratification into sun/shade leaves, as discussed below. The increased stratification of the canopy from 2010 to 2012 is also reflected in the much larger variability of GEP rates, with larger standard deviations in 2012 compared with 2010 (dashed error bars, Figure 5).

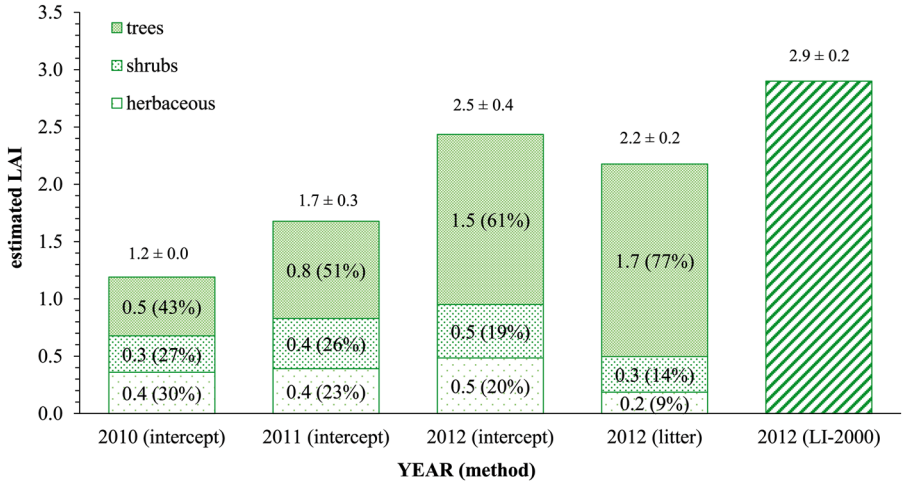

Figure 3. Total LAI and its composition at the clearcut site from 2010 to 2012. Estimates shown have been derived from the line-intercept method, except for the year 2012, where estimates from the litter-trap method and from measurements with the LAI-2000 were also available and are shown. The values inside each bar represent the LAI of the corresponding vegetation group (i.e., herbs, shrubs and trees) and the percent values in brackets represent the percent contribution of the subgroup's LAI to the total estimated site's LAI. The trends in LAI reflect the trends in ground cover and vegetation composition shown in Figure 2. The greatest change in LAI occurred due to the expansion of tree canopy, which begins to shade out herbs and shrubs.

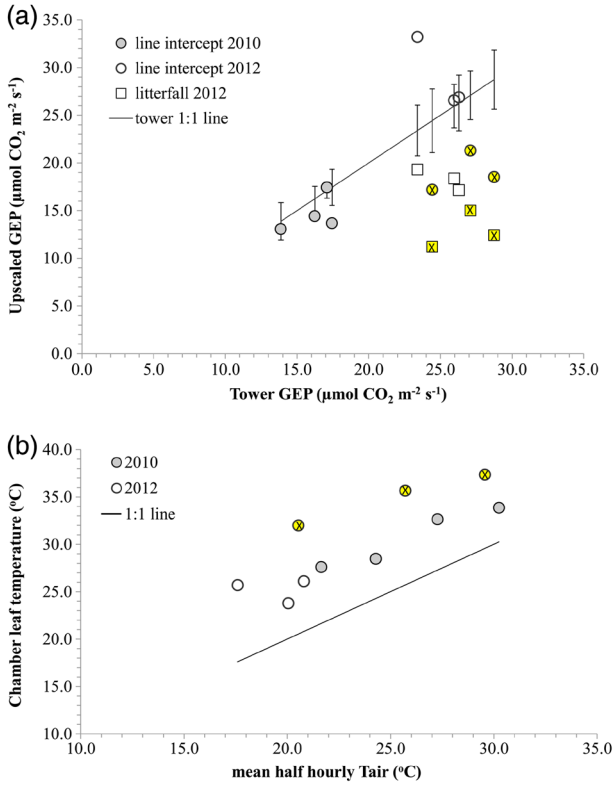

Figure 4. (a) Chamber-based upscaled-GEP vs. EC measured instantaneous GEP for the two upscaling methods (line-intercept and litterfall) and 2 years of observation (2010 and 2012); (b) above-canopy air temperature (Tair) plotted vs. leaf temperature inside the chamber sampled on the same day as the corresponding fluxes presented in (a). Outliers (filled symbols with an x mark) indicate conditions when the temperature of chamber-measured leaves substantially exceeded air temperatures recorded on the tower. Overall, chamber temperatures were higher vs. tower-recorded temperatures.

Overall, upscaled-GEP values were comparable to tower GEP values (Figures 4 and 5), allowing us to use the upscaled curves to quantitatively test whether the interannual changes in vegetation composition or expanding LAI dominated the rise in the GEP. To do so, we compared the true leaf-upscaled results for 2012 with those we would have obtained if either LAI or vegetation composition had remained fixed at the values recorded in 2010 (Figure 6). Changing vegetation composition was not capable of explaining the rise in GEP from 2010 to 2012, but changing LAI was (Figure 6). Using 2010 vegetation composition and 2012 LA in upscaling leaf-level fluxes resulted in upscaled values almost identical to the true 2012 upscaled curve (Figure 6). In contrast, using 2012 vegetation composition, but 2010 leaf area, yielded upscaled light-response values much lower than those observed in 2012 (Figure 6).

Discussion

Gross ecosystem productivity recovery after the clearcut

Growing season (May to September) GEP increased steadily at the site from 2009 to 2012, as was first reported by Williams et al. (2014). By 2012, growing season GEP (1351 g C m^{-2} $year^{-1}$) was comparable to that measured at the nearby reference mature deciduous stand, monitored by the Harvard Forest Environmental Monitoring Station (EMS). Urbanski et al. (2007) reported GEP at the EMS site averaging 1350 ± 160 g C m^{-2} $year^{-1}$ for the years 1992–2004, for the period of April to October, and LAI values of ~5 m^2 m^{-2}. Interestingly, when we compared LAI-normalized GEP for the 3 years of our study at the clearcut with that of the last 4 years of data presented in Urbanski et al. (2007), we observed that the

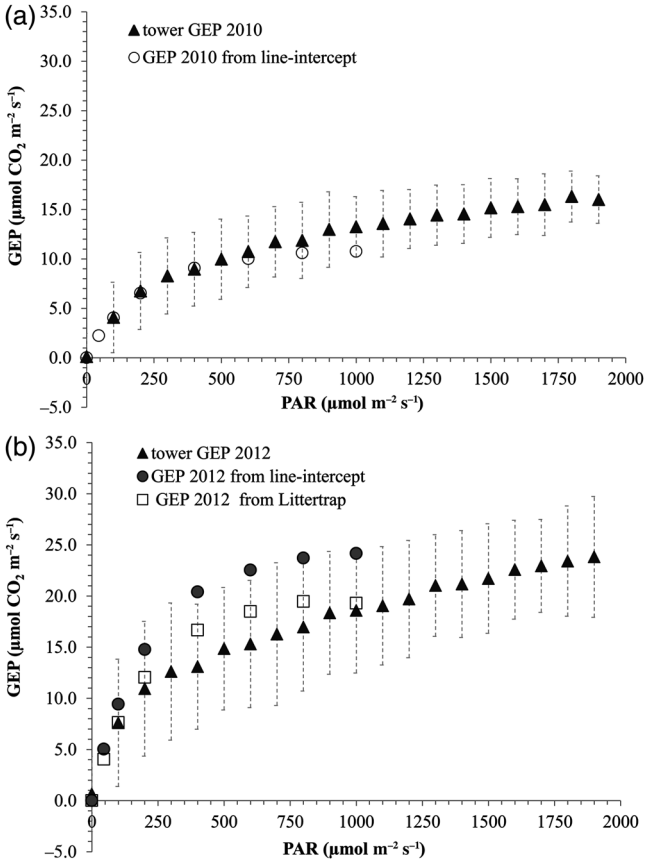

Figure 5. GEP light-response curves derived from EC data and upscaling of leaf-chamber data, using either the line-intercept method or the litterfall method to estimate LAI. Values shown are averages for measurements from May to September for (a) year 2010 and (b) year 2012. Error bars represent the standard deviation around the mean GEP values for the tower, corresponding to each light level. In both years, the upscaled values reflect well the initial rise and slope and slope of the tower values. However, differences show up in the saturating part of the curve. Overall, the canopy (i.e., tower GEP) EC measurements never reached saturation, compared with enclosed leaves (upscaled GEP). In 2012 our upscaled values were higher compared with EC values at intermediate light levels, likely due to our inability to account for shaded leaves.

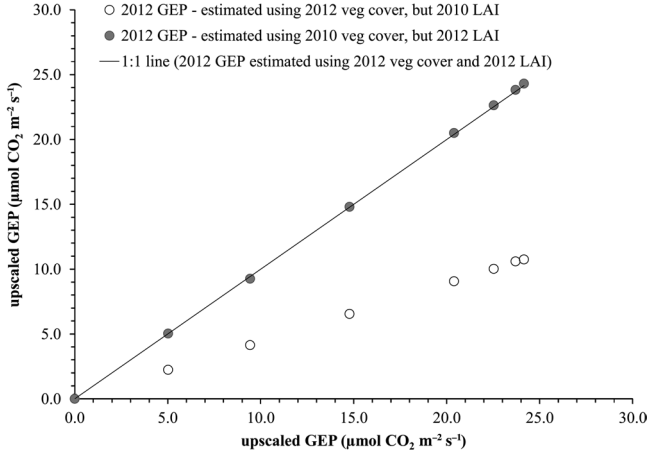

Figure 6. Here we show what our upscaled GEP for 2012 would look like had we used 2010 vegetation composition but 2012 LAI to upscale the chamber measurements (filled circles). Similarly, we also plot the result upscaled using 2012 vegetation composition but 2010 LAI (open circles). Clearly, changing the composition does not make much of a difference in our upscaled values—they are almost identical to the 1 : 1 line. In contrast, changing LAI to that of 2010 reduced the upscaled values well below the 1 : 1 line. Data points represent values for each sampled light level (from the upscaled GEP-PAR curves, as shown in Figure 5).

mature stand's GEP per unit LA (i.e., GEP/LAI) is relatively constant and lower (range of 286–330), while that at the clearcut decreased with age in an approach to that of the mature stand (i.e., 783, 644, 540 for years 2009, 2010 and 2012, respectively).

The large presence of pin cherry at the clearcut site, but not at the mature EMS site, might contribute to the GEP at the clearcut site being comparable to that at the neighboring mature forest, despite lower LA within the clearcut site. Pin cherry has been reported to retain green foliage longer and to sustain a longer photosynthetically active season compared with birch (*Betula* sp.), beech (*Fagus* sp.), and red maple, which were more prevalent at the mature site (Amthor et al. 1990). We have also found pin cherry to have the highest rate of photosynthesis per unit LA among the species studied here, which could also contribute to the rapid rise in GEP possibly even surpassing that in the neighboring mature forest.

The recovery of GEP at our clearcut site was rapid compared with past studies in humid temperate regions of the USA. For example, during the first year after clearcutting at Coweeta Hydrological Station in North Carolina, the site's annual productivity was only 22% of that in a neighboring mature undisturbed stand (Boring et al. 1981). Similarly, when the clearcut watershed at Hubbard Brook in New Hampshire was allowed to regenerate naturally, the above-ground productivity was 5% of that observed in an adjacent undisturbed stand in Year 1, ~25% in Year 2 and 63% in Year 4 (Likens et al. 1978). We note, however, that although the studies mentioned above were done in similar ecosystems and climate to ours, they used different methods to determine annual productivity, relying on biometric estimates that could miss some of the gross photosynthetic uptake.

Several studies have used the EC method to follow sites for multiple years immediately following a clearcut. For example, Takagi et al. (2009) measured GEP in a temperate mixed-wood forest in Japan before clearcutting and continued measurements 3 years post-clearcut, when the site was planted with larch trees. The recovery of their stand was similar to ours in terms of GEP. By the third season post-clearcut, their site's GEP recovered to ~70% of GEP in the pre-harvest stand (cf. plantation at 3 years post-clearcut GEP of 1014 g C m^{-2} $year^{-1}$ vs. mature mixed-wood stand GEP of 1439 g C m^{-2} $year^{-1}$). They suggest that much of the recovery was likely due to the largely undisturbed bamboo understory left at the site during

harvesting (Takagi et al. 2009). Despite the large increase in GEP over the years, Takagi et al. (2009) reported a pre-harvest stand PAI of 3.2–4.6 and a 3 years post-harvest PAI of 1.28. In another study, which used the EC method to monitor post-clearcut regeneration, Humphreys et al. (2005) reported a recovery of GEP in a coastal Douglas fir plantation on Vancouver Island, BC, Canada. Their stand was a plantation prior to harvest and was replanted with the same species post-harvest, unlike in Takagi et al. (2009) and in the present study. The rate of recovery of GEP of the Canadian stand was slower compared with what we observed at our site. In the third year of recovery, the GEP at the plantation (640 g C m^{-2} $year^{-1}$; Humphreys et al. 2005) was only about a third of the GEP of a neighboring mature Douglas fir stand (2158 ± 163 g C m^{-2} $year^{-1}$; Krishnan et al. 2009). Leaf area index recovery was similar to that of GEP: by the third year of recovery, the clearcut's LAI was 2.53 ± 0.13, compared with that of the neighboring mature stand with an LAI of 7.3 (Krishnan et al. 2009). Humphreys et al. (2005) noted that most of the LAI recovery was due to the recovery of herbs and shrubs in the understory and that the growth of planted seedlings was relatively slow. The difference in tree species present at the west-coast regenerating plantation, compared with our pin-cherry-dominated stand, could be one reason for the discrepancy in annual GEP recovery between our site and that of Humphreys et al. (2005). Finally, in a comparison of a mature (65-year-old) hardwood forest to that of a 3-year-old clearcut located in WI, USA, Noormets et al. (2007) reported a 66% increase in GEP, but only a 20% increase in LAI (i.e., their clearcut had a GEP of 697 ± 3.8 g C m^{-2} from May to October, compared with the mature stand's GEP of 1047 ± 5.4 g C m^{-2}, while LAI at the clearcut was 0.8 ± 0.6 vs. 3.9 ± 0.6 at the mature stand). The synthesis by Amiro et al. (2010) reports that GEP recovery often continues over a period of 20–30 years following a disturbance. While it remains to be seen if GEP continues to rise at our site, the fact that it has already achieved rates of productivity comparable to that measured in the adjacent mature forest highlights the resilience of vegetation recovery at our site.

Attributing the observed increase in GEP to mechanisms

We observed a positive linear relationship between LAI and GEP at our site that unfolded over the first 4 years post-clearing. This was similar to the pattern reported by Humphreys et al. (2005) in their Douglas fir clearcut. Coursolle et al. (2012) also reported a strong positive and linear relationship in a boreal clearcut over the course of a 10-year recovery. The estimated LAI at our site for the year 2012 was about half of the estimated LAI for the neighboring EMS stand, which we use as a reference mature stand. Urbanski et al. (2007) reported LAI values between 4.5 and 5.6 m^2 m^{-2} for the period from 1998 to 2004 for the EMS stand. By the second growing season, the LAI at our clearcut site was 1.2 m^2 m^{-2}, which was comparable to past studies in other northeast clearcut areas. For example, the LAI of the Coweeta clearcut was 1.3 m^2 m^{-2} after the first year and this was lower relative to the local undisturbed site with an LAI of 5 m^2 m^{-2} (Boring et al. 1981), similar to the 2010 LAI of our clearcut site compared with the mature EMS stand at Harvard Forest. The rise in LAI at our site over the 4 years since the clearcut resembled the rise in LAI at Hubbard Brook clearcut, where LA rose from 1.1 m^2 m^{-2} in Year 1 to 5.5 m^2 m^{-2} in Year 4 after a clearcut (Marks 1974). In the early stages of a pine forest regeneration in southeastern USA, Bracho et al. (2012) attributed increases in their stand's carbon assimilation to expansion of LAI. In the first 4 years of recovery, their site's GEP was almost that of the 25-year-old stand (cf. 2458 vs. 2621 g C m^2 $year^{-1}$), while LAI was only a sixth of that of the older stand (i.e., 0.99 vs. 6.23 m^2 m^{-2}).

We also observed large changes in vegetation composition over the 3 years, potentially introducing a trend in leaf-level photosynthetic capacity (Waring et al. 1995, Bassow and Bazzaz 1997) that could have also contributed to the rise in GEP. Trees increased in dominance from 2009 to 2012. However, by year 2012, the two dominant species were Allegheny blackberry and pin cherry. Both of these are considered pioneer species, which grow after a disturbance in local deciduous forests in the USA (Marks 1974, Amthor et al. 1990, Reich et al. 1990). Photosynthetic capacity for early-successional species tends to be high compared with late-successional species (Bazzaz 1979).

Interestingly, leaf-level photosynthetic capacity did not vary significantly between species in almost all cases. It is possible that our sampling was not intense enough to capture any variability. In a separate study at the site, Dillen et al. (2012) reported seasonal variability in leaf physiological traits and among species from spring to fall, with the least seasonal variability in summertime (most of our measurements in 2012 were taken in June to July). Specific leaf area did differ statistically between the three major groups, reflecting the light environment to which each group is adapted. Herbaceous species often find themselves hidden below shrubs and trees, growing in more shaded environments, so they tend to maximize their LA to weight (i.e., photosynthetic area per gram of tissue). However, variation in SLA did not translate into variation in photosynthetic capacity.

Red maple presented a noticeable exception to the above-mentioned broad patterns, with low photosynthetic capacity and low leaf nitrogen content relative to the other species. Red maples are known to be a shade-tolerant species, with low resource requirements and relatively low photosynthetic capacity (Bassow and Bazzaz 1997, Abrams 1998). In a comparison of leaf traits of a regenerating oak forest in Wisconsin, Reich et al. (1990) also reported leaf nitrogen of red maple trees to be lower compared with that of blackberry (*Rubus* sp.) and black cherry (*P. serotina*). At our site, red maples, which

are commonly understood to be mid-to-late-successional species, were second only to pin cherries in their contribution to the percent vegetation cover by trees in 2012. Their regeneration was partly due to resprouting stumps at the site. Even so, the low photosynthetic capacity of red maple was inconsequential to ecosystem-scale productivity at the clearcut site studied here. However, it is expected to gradually rise, as red maple becomes canopy dominant, which is typical in the mature stage of forest succession in this region.

Looking between years, leaf-level photosynthetic capacity did not differ between 2010 and 2012 for the species measured in both years. This runs contrary to some past studies that have shown how, as deciduous forests grow and develop, photosynthetic capacity of individuals may change with age (Wilson et al. 2001, Augspurger and Bartlett 2003). It could be that during the 4 years post-clearcut, the competition for light and nutrients is still only modest and/or that the vegetation is still relatively young, but this remains to be seen with continued monitoring.

Finally, we should mention some of the challenges that emerged in our tower- to chamber-based GEP comparisons. Though direct comparison of leaf-upscaled and tower-based instantaneous GEP showed good agreement overall, the tower-based response curves did not exhibit the same saturation at intermediate-to-high light levels as seen in leaf-based light-response curves. The tower reflects the whole canopy, which is composed of fully sun-lit and shaded leaves, while our measurements were almost exclusively based on well-lit leaves. The regenerating forest studied here had already developed a three-layer canopy structure by 2012 (3 years following clearing), with herbs at the bottom, shaded by shrubs, which were in turn shaded by a tree layer consisting of seedlings and saplings (with a mean height of 1.4 ± 0.8 m, but reaching a maximum height of over 4 m). The trend in the GEP/LAI ratio at our clearcut, mentioned above, is also suggestive of the development of layers in the canopy and the increased presence of shaded leaves, since for every extra LAI unit increase, our GEP did not increase proportionately (instead it increased at a much lower rate). Such layering could give rise to vertical variation in leaf physiology and photosynthetic capacity (Ellsworth and Reich 1993, Gill et al. 1998, Augspurger and Bartlett 2003). However, we were unable to test the relative contribution of shade and sun-lit leaves to GEP at our site, due to logistical constraints on the amount of measurements we could take in one growing season. When we compared our chamber-measured A_{max} values with those reported by Abrams (1998) for shaded understory species in eastern North America, we found our values to be higher, suggesting that the vegetation sampled at our clearcut site was representative of sun-lit foliage (i.e., compare Table 1 with values from Abrams (1998): *A. rubrum* range 2.7–4.4 μmol CO_2 m^{-2} s^{-1}; *P. pennsylvanica* 5.0 μmol CO_2 m^{-2} s^{-1}; *P. serotina* 3.7 μmol CO_2 m^{-2} s^{-1}; *Q. rubra* 2.4–7.4 μmol CO_2 m^{-2} s^{-1}). Sun-/shade-leaf emergence due to increased stratification could also cause the switch between light- and Rubisco-limited photosynthesis to occur at different points in the canopy. This reinforces the importance of sub-canopy light limitation in mediating the GEP–LAI relationship at this site as it grows further and matures.

Additionally, the tower-based curve was generated by aggregating all data for a given PAR level. This inevitably included GEP signals from early mornings, late evenings and cloudy days—times when the leaf and canopy physiological response to light might be different from that measured during midday, because of bias in other environmental conditions that are coincident (e.g., air temperature, humidity, light quality or vegetation hydration). Indeed, ~95% of the data at PAR levels ≤250 μmol were from measurements taken before 8:00 or after 18:00 h, with the remaining daytime measurements falling on either rainy or overcast days (data not shown).

Another challenge we faced was methodological uncertainty in LAI estimates. There were a few reasons to believe that the LAI from the litter-trap method is too low. First, logistical constraints precluded us from collecting litterfall throughout the growing season. In addition, we did not capture low-stature herbs, such as the Canadian May lily or several grasses, due to the litter traps being elevated just above the ground. Another possible cause for underestimation is litter loss due to wind blowing litter out of the traps between sampling dates. Even so, the relative contributions across plant functional groups remained similar between the methods (see Figure S5 available as Supplementary Data at *Tree Physiology* Online). And despite these challenges, we obtained good overall agreement between leaf-upscaled and flux-tower estimates of instantaneous GEP, as well as the maximum GEP at high light levels, which lends confidence to the use of leaf-based upscaling to attribute the multi-year rise in GEP to vegetation compositional shifts vs. expanded LA.

Conclusions

The multi-year rise in GEP with early regrowth following clearcutting was clearly attributed to the expansion of LA rather than a change in vegetation composition. Sizeable changes in the relative abundance of species were masked by remarkably similar leaf physiological attributes for a range of vegetation types present in the early-successional environment. Comparison of upscaled leaf-chamber estimates with EC-based estimates of the light-response curve revealed a broad consistency in both maximum photosynthetic capacity and quantum yield efficiency. However, differences in the shape of the curves suggested the need for a more sophisticated upscaling that considers a multi-layered canopy with both sun- and shade-leaf contributions. Seasonality of leaf physiological traits should also be considered in similar future studies. The

approaches presented here demonstrate how chamber- and ecosystem-scale measurements of gas exchange can be usefully blended to draw conclusive inferences about changes in ecosystem processes over time in a highly dynamic environment, such as the post-clearcut setting studied here.

Supplementary data

Supplementary data are available at *Tree Physiology* online.

Acknowledgments

The authors are very grateful to and thank the many dedicated field research assistants, who endured challenging field conditions: Thorsen Akerley, Katherine Chute, Crystal Garcia, Bardan Ghimire, Krittika Govil, Alex Kappel, Angela Marshall, Marcus Pasay, Paul Quackenbush and Graham Twibell. They also thank their colleagues at Harvard Forest, for providing technical or lab expertise or lending equipment: Manisha Pattel for CN leaf analysis and lab help; Mark VanScoy for technical support and lab help; John Wisnewski and woods crew for logistical support; Aaron Ellison for use of LI-6400; Kristina Stinson for use of LI-3000; David Foster, Audrey Barker-Plotkin and the Harvard Forest Long-Term Ecological Research Site (LTER) for assistance with site selection.

Conflict of interest

None declared.

Funding

Major financial support for this work came from research funds awarded to C.A.W. by Clark University, and also from NASA Terrestrial Ecology award NNX10AR68G (2N041), and the 2010–2011 Albert, Norma and Howard Geller '77 Endowed research Awards for Projects Relating to Sustainability (G.P. Marsh Institute, Clark University). Many of our undergraduate summer research assistants were supported by the Research Experience for Undergraduates Site award to the Harvard Forest LTER site (NSF Award #0620443). In different years, the students were supported by DOE TCP—DE-SC0004985 (2011), NSF REU Site—DBI-1003938 (2012) and NASA NICE—NNX10AT52A (2013). In addition, we acknowledge financial support from the NSF LTER IV grant: Integrated Studies of the Drivers, Dynamics and Consequences of Landscape Change in New England (DEB-0620443), providing core logistical support that aided our research.

References

Abrams MD (1998) The red maple paradox. BioScience 48:355–364.

Amiro BD, Todd JB, Wotton BM, Logan KA, Flannigan MD, Stocks BJ, Mason JA, Martell DL, Hirsch KG (2001) Direct carbon emissions from Canadian forest fires, 1959–1999. Can J For Res 31: 512–525.

Amiro BD, Barr AG, Barr JG et al. (2010) Ecosystem carbon dioxide fluxes after disturbance in forests of North America. J Geophys Res 115:G00K02.

Amthor JS, Gill DS, Bormann FH (1990) Autumnal leaf conductance and apparent photosynthesis by saplings and sprouts in a recently disturbed northern hardwood forest. Oecologia 84:93–98.

Augspurger CK, Bartlett EA (2003) Differences in leaf phenology between juvenile and adult trees in a temperate deciduous forest. Tree Physiol 23:517–525.

Bassow SL, Bazzaz FA (1997) Intra-and inter-specific variation in canopy photosynthesis in a mixed deciduous forest. Oecologia 109:507–515.

Bazzaz FA (1979) The physiological ecology of plant succession. Annu Rev Ecol Syst 10:351–371.

Becker DR, Skog K, Hellman A, Halvorsen KE, Mace T (2009) An outlook for sustainable forest bioenergy production in the Lake States. Energy Policy 37:5687–5693.

Beer C, Reichstein M, Tomelleri E et al. (2010) Terrestrial gross carbon dioxide uptake: global distribution and covariation with climate. Science 329:834–838.

Bonan GB (2008) Forests and climate change: forcings, feedbacks, and the climate benefits of forests. Science 320:1444–1449.

Bond-Lamberty B, Peckham SD, Ahl DE, Gower ST (2007) Fire as the dominant driver of central Canadian boreal forest carbon balance. Nature 450:89–92.

Boose E (2001) Fisher meteorological station at Harvard Forest since 2001. Harvard Forest Data Archive: HF001. [Database] http://harvardforest.fas.harvard.edu/data-archive (18 June 2014, date last accessed).

Boring LR, Monk CD, Swank WT (1981) Early regeneration of a clearcut southern Appalachian forest. Ecology 65:1244–1253.

Bracho R, Starr G, Gholz HL, Martin TA, Cropper WP, Loescher HW (2012) Controls on carbon dynamics by ecosystem structure and climate for southeastern US slash pine plantations. Ecol Monogr 82:101–128.

Canadian Carbon Program (2011) In: Coursolle C (ed) Ecosystems in flux: carbon, climate and disturbance in Canadian forests and peatlands. Canadian Carbon Program, Quebec, QC, Canada, pp 10–11.

Coursolle C, Giasson MA, Margolis HA, Bernier PY (2012) Moving towards carbon neutrality: CO_2 exchange of a black spruce forest ecosystem during the first 10 years of recovery after harvest. Can J For Res 42:1908–1918.

Denman KL, Brasseur G, Chidthaisong A et al. (2007) Couplings between changes in the climate system and biogeochemistry. In: Solomon S, Qin D, Manning M, Chen Z, Marquis M, Averyt KB, Tignor M, Miller HL (eds) Climate change 2007: the physical science basis. Contribution of Working Group I to the Fourth Assessment Report of the Intergovernmental Panel on Climate Change. Cambridge University Press, Cambridge, UK.

Dillen SY, de Beeck MO, Hufkens K, Buonanduci M, Phillips NG (2012) Seasonal patterns of foliar reflectance in relation to photosynthetic capacity and color index in two co-occurring tree species, *Quercus rubra* and *Betula papyrifera*. Agric For Meteorol 160:60–68.

Dixon RK, Krankina ON (1993) Forest fires in Russia: carbon dioxide emissions to the atmosphere. Can J For Res 23:1042–1049.

Ellsworth DS, Reich PB (1993) Canopy structure and vertical patterns of photosynthesis and related leaf traits in a deciduous forest. Oecologia 96:169–178.

Everham EM, Brokaw NVL (1996) Forest damage and recovery from catastrophic wind. Bot Rev 62:113–185.

Finkral AJ, Evans AM (2008) The effects of a thinning treatment on carbon stocks in a northern Arizona ponderosa pine forest. For Ecol Manage 255:2743–2750.

Food and Agriculture Organization (FAO) of the United Nations (2006) Global forest resources assessment 2005: progress towards sustainable forest management. Food and Agriculture Organization, Rome, Italy.

Gill DS, Amthor JS, Bormann FH (1998) Leaf phenology, photosynthesis, and the persistence of saplings and shrubs in a mature northern hardwood forest. Tree Physiol 18:281–289.

Goodale CL, Apps MJ, Birdsey RA et al. (2002) Forest carbon sinks in the northern hemisphere. Ecol Appl 12:891–899.

Hanson PJ, McRoberts RE, Isebrands JG, Dixon RK (1987) An optimal sampling strategy for determining CO_2 exchange rate as a function of photosynthetic photon flux density. Photosynthetica 21:98–101.

Hicke JA, Allen CD, Desai AR et al. (2012) Effects of biotic disturbances on forest carbon cycling in the United States and Canada. Glob Change Biol 18:7–34.

Hooper MC, Arii K, Lechowicz MJ (2001) Impact of a major ice storm on an old-growth hardwood forest. Can J Bot 79:70–75.

Humphreys ER, Black TA, Morgenstern K, Li Z, Nesic Z (2005) Net ecosystem production of a Douglas-fir stand for 3 years following clearcut harvesting. Glob Change Biol 11:450–465.

Jandl R, Lindner M, Vesterdal L, Bauwens B, Baritz R, Hagedorn F, Johnson DW, Minkkinen K, Byrne KA (2007) How strongly can forest management influence soil carbon sequestration? Geoderma 137:253–268.

Keenan RJ, Kimmins JP (1993) The ecological effects of clear-cutting. Environ Rev 1:121–144.

Kielland K, Bryant JP (1998) Moose herbivory in taiga: effects on biogeochemistry and vegetation dynamics in primary succession. Oikos 82:377–383.

Kirby KR, Potvin C (2007) Variation in carbon storage among tree species: implications for the management of a small-scale carbon sink project. For Ecol Manage 246:208–221.

Kittredge D, Foster D, McDonald R (2009) Massachusetts timber harvesting study. Harvard Forest Data Archive: HF080. [Database] http://harvardforest.fas.harvard.edu/data-archive (18 June 2014, date last accessed).

Kozlowski TT (1980) Impacts of air pollution on forest ecosystems. BioScience 30:88–93.

Krishnan P, Black TA, Jassal RS, Chen B, Nesic Z (2009) Interannual variability of the carbon balance of three different-aged Douglas-fir stands in the Pacific Northwest. J Geophys Res 114:G04011.

Lasslop G, Reichstein M, Papale D, Richardson AD, Arneth A, Barr A, Stoy P, Wohlfahrt G (2010) Separation of net ecosystem exchange into assimilation and respiration using a light response curve approach: critical issues and global evaluation. Glob Change Biol 16:187–208.

Likens GE, Bormann FH, Pierce RS, Reiners WA (1978) Recovery of a deforested ecosystem. Science 199:492–496.

Marks PL (1974) The role of pin cherry (*Prunus pensylvanica* L.) in the maintenance of stability in northern hardwood ecosystems. Ecol Monogr 44:73–88.

Myneni RB, Dong J, Tucker CJ, Kaufmann RK, Kauppi PE, Liski J, Zhou L, Alexeyev V, Hughes MK (2001) A large carbon sink in the woody biomass of Northern forests. Proc Natl Acad Sci USA 98:14784–14789.

Nemani RR, Keeling CD, Hashimoto H, Jolly WM, Piper SC, Tucker CJ, Myneni RB, Running SW (2003) Climate-driven increases in global terrestrial net primary production from 1982 to 1999. Science 300:1560–1563.

Noormets A, Chen J, Crow TR (2007) Age-dependent changes in ecosystem carbon fluxes in managed forests in northern Wisconsin, USA. Ecosystems 10:187–203.

NRCS (2010) Soil Survey Geographic (SSURGO) Database for Worcester County, Massachusetts. Natural Resources Conservation Service, USDA. http://websoilsurvey.sc.egov.usda.gov (19 June 2014, date last accessed).

Oren R, Ellsworth DS, Johnson KH et al. (2001) Soil fertility limits carbon sequestration by forest ecosystems in a CO_2-enriched atmosphere. Nature 411:469–472.

Pregitzer KS, Euskirchen ES (2004) Carbon cycling and storage in world forests: biome patterns related to forest age. Glob Change Biol 10:2052–2077.

Reich PB, Abrams MD, Ellsworth DS, Kruger EL, Tabone TJ (1990) Fire affects ecophysiology and community dynamics of central Wisconsin oak forest regeneration. Ecology 71:2179–2190.

Reichstein M, Falge E, Baldocchi D et al. (2005) On the separation of net ecosystem exchange into assimilation and ecosystem respiration: review and improved algorithm. Glob Change Biol 11: 1424–1439.

Rustad LE, Campbell JL (2012) An ice storm manipulation experiment in a northern hardwood forest. Can J For Res 42:1810–1818.

Sharkey TD, Bernacchi CJ, Farquhar GD, Singsaas EL (2007) Fitting photosynthetic carbon dioxide response curves for C3 leaves. Plant Cell Environ 30:1035–1040.

Smith WB, Miles PD, Perry CH, Pugh SA, Forest Resources of the United States, 2007 (2009) Forest resources of the United States. Gen. Tech. Rep. WO-78. USDA, Forest Service, Washington Office, Washington, DC.

Takagi K, Fukuzawa K, Liang N et al. (2009) Change in CO_2 balance under a series of forestry activities in a cool-temperature mixed forest with dense undergrowth. Glob Change Biol 15:1275–1288.

Twibell G, Williams CA (2011) The use of silvicultural treatments in Massachusetts: characteristics, impacts, and motivations associated with various forest harvesting methods, MA thesis, Clark University, Worcester, MA.

Urbanski S, Barford C, Wofsy S et al. (2007) Factors controlling CO_2 exchange on timescales from hourly to decadal at Harvard Forest. J Geophys Res 112:G02020. doi:10.1029/2006JG000293.

Vanderhoof M, Williams CA, Pasay M, Ghimire B (2013) Controls on the rate of CO_2 emission from woody debris in clearcut and coniferous forest environments of central Massachusetts. Biogeochemistry 114:299–311.

Waring RH, Law BE, Goulden ML, Bassow SL, McCreight RW, Wofsy SC, Bazzaz FA (1995) Scaling gross ecosystem production at Harvard Forest with remote sensing: a comparison of estimates from a constrained quantum-use efficiency model and eddy correlation. Plant Cell Environ 18:1201–1213.

Williams CA, Vanderhoof M, Khomik M, Ghimire B (2014) Post-clearcut dynamics of carbon, water and energy exchanges in a mid-latitude temperate, deciduous broadleaf forest environment. Glob Change Biol 20:992–1007.

Wilson KB, Baldocchi DD, Hanson PJ (2001) Leaf age affects the seasonal pattern of photosynthetic capacity and net ecosystem exchange of carbon in a deciduous forest. Plant Cell Environ 24:571–583.